

## Hybrid ZnO/III-nitride light-emitting diodes: modelling analysis of operation

K. A. Bulashevich<sup>1,2</sup>, I. Yu. Evstratov<sup>3</sup>, and S. Yu. Karpov<sup>1,3\*</sup>

<sup>1</sup> STR, Inc., P.O. Box 70604, Richmond, VA 23255-0604, USA

<sup>2</sup> Ioffe Physico-Technical Institute RAS, 26 Polytechnicheskaya, St.Petersburg, 194021 Russia

<sup>3</sup> Soft-Impact, Ltd., P.O. Box 83, St.Petersburg, 194156 Russia

Received 4 May 2006, revised 11 October 2006, accepted 13 October 2006

Published online 5 January 2007

PACS 85.60.Bt, 85.60.Jb, 73.40.–c, 78.66.Hf.

Using simulations, we have analysed basic mechanisms of hybrid II-O/III-N light-emitting diode operation. Factors largely affecting the internal quantum efficiency of hybrid single- and double heterostructures, including operation temperature, are examined in detail.

Preprint 2006

**Introduction** Due to a direct bandgap of 3.37 eV and a high exciton binding energy of ~60 meV, ZnO has gained substantial interest as a promising material for highly efficient UV light-emitting diodes (LEDs) and laser diodes (LDs) based on exciton recombination [1]. Availability of native ZnO substrates and wurtzite MgZnO and CdZnO alloys with a bandgap varying from ~2 eV to ~4 eV makes feasible growth of low-dislocation heterostructures necessary for LED and LD fabrication. Additional advantage of ZnO is the applicability of low-temperature epitaxy and wet etching for device processing. However, development of the ZnO-based light emitters is largely impeded by the lack of reliable *p*-doping technology [2]. Though much progress has been made in recent years to attain reliable *p*-doping of ZnO, an alternative approach is suggested based on hybrid LED heterostructures combining *p*-doped III-nitride and *n*-doped II-oxide epitaxial materials closely lattice-matched with each other. First hybrid single-heterostructure (SHS) and double-heterostructure (DHS) LEDs have been already demonstrated [3–5].

The in-plane lattice mismatch between ZnO and GaN is of ~1.9%, even smaller than between GaN and AlN (~2.4%), which is favourable for getting a high-quality ZnO/GaN interface with reduced surface recombination. The GaN/ZnO heterojunction is known to form a type-II band alignment [6] with the valence band offset ~0.8–1.0 eV. Having wurtzite crystal symmetry, ZnO, as well as MgZnO and CdZnO alloys, exhibit both piezo- and spontaneous electric polarization. All these factors are important for engineering of hybrid LED heterostructures and determine specific features of their operation.

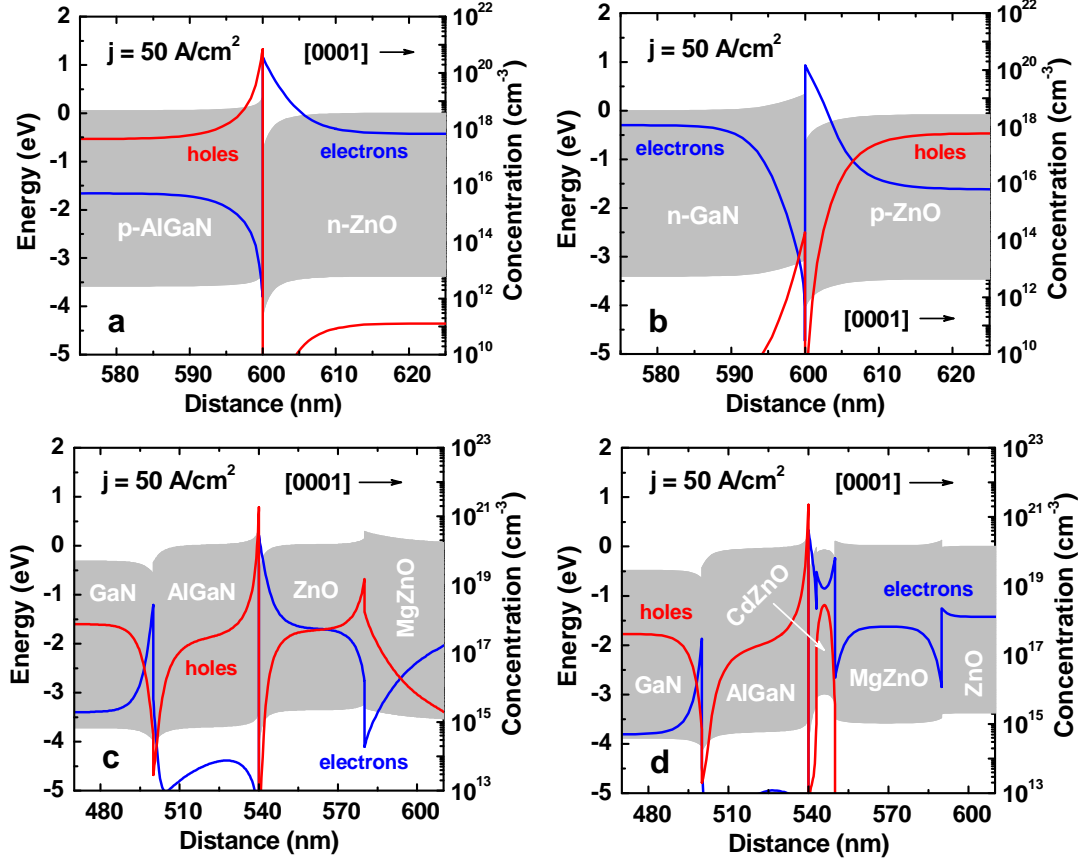
Using simulations, we consider a number of typical hybrid SHS and DHS LEDs and investigate into basic mechanisms of their operation. The simulation model has been described in detail elsewhere [7]. The materials properties of III-nitrides and II-oxides have been chosen close to those recommended in [8] and [4], respectively.

**Single-heterostructure LEDs** We consider first two hybrid SHS LEDs suggested in [3] and [9]. The structure reported in [3] consists of a 0.8  $\mu\text{m}$  *p*-Al<sub>0.12</sub>Ga<sub>0.88</sub>N layer grown by hydride vapor-phase epitaxy followed by a 1.0  $\mu\text{m}$  *n*-ZnO grown by chemical vapor deposition enhanced by the RF-discharge plasma. The hole and electron concentrations in the layers were estimated as  $\sim 5 \times 10^{17} \text{ cm}^{-3}$  and  $\sim 7 \times 10^{17} \text{ cm}^{-3}$ , respectively. The structure from Ref.[9] has the inverted sequence of doped layers: a 1.6  $\mu\text{m}$  *n*-GaN layer ( $n = 1.2 \times 10^{18} \text{ cm}^{-3}$ ,  $\mu_n = 200 \text{ cm}^2/\text{V}\cdot\text{s}$ ) grown by MOVPE, and a 0.4  $\mu\text{m}$  *p*-ZnO layer ( $p = 6.7 \times 10^{17} \text{ cm}^{-3}$ ,

---

\* Corresponding author: e-mail: karpov@semitech.us, Phone: +1 804 740 8314, Fax: +1 804 740 3814

$\mu_p = 1.4 \text{ cm}^2/\text{V}\cdot\text{s}$ ) deposited on the top of  $n$ -GaN by the RF-magnetron sputtering. Both structures are assumed to have Ga/Zn-polarity and to be relaxed because of sufficient thickness of epitaxial layers. Thus only the spontaneous polarization can contribute to the interface charges. The threading dislocation density (TDD) of  $10^9 \text{ cm}^{-2}$  is considered in simulations as the value typical of III-nitride heterostructures grown on conventional sapphire or SiC substrates.



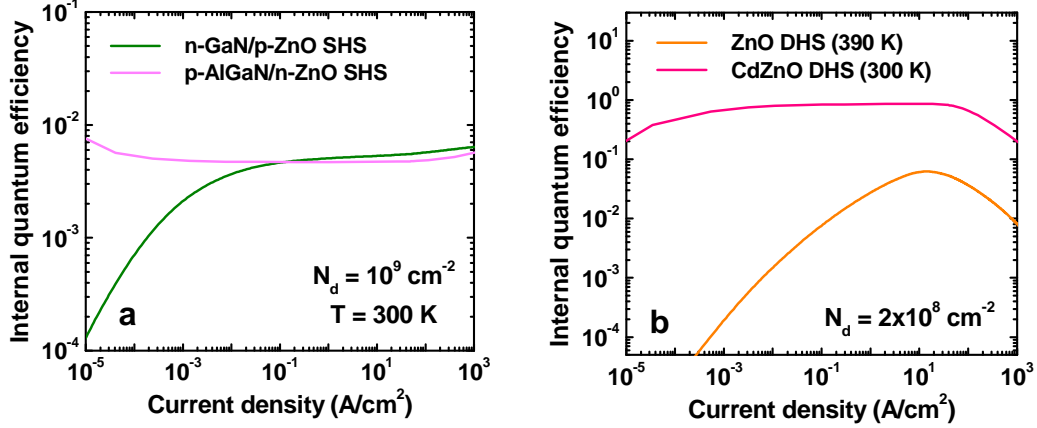
**Fig.1** Band diagrams (grey shadow) and distributions of carrier concentrations (lines) in AlGaIn/ZnO SHS (a), inverted GaN/ZnO SHS (b), ZnO DHS (c) and CdZnO DHS (d) light-emitting diodes.

Fig.1a,b compares the band diagrams and distributions of carrier concentrations in the AlGaIn/ZnO and inverted GaN/ZnO LED structures at the current density of  $50 \text{ A/cm}^2$ . Due to a type-II band alignment and a positive interface polarization charge, electrons and holes are confined in the local potential wells adjacent to the AlGaIn/ZnO heterojunction, where their concentrations are at least two orders of magnitude higher than in the heterostructure bulk (Fig.1a). This enables tunnel radiative recombination of the confined carriers resulting in the emission spectra peaked at 410–430 nm, in spite of a small overlap of the electron and hole wave functions (see [10] for detailed analysis). In the GaN/ZnO LED with the inverted sequence of  $n$ - and  $p$ -regions electrons and holes are also confined at the interface but in the  $p$ -ZnO and  $n$ -GaN, respectively. This leads to a much lower hole concentration at the interface (Fig.1b). Nevertheless, the tunnel emission spectrum calculated for this heterostructure fits well the measured one, peaked at  $\sim 410 \text{ nm}$ , which could be attributed neither to  $n$ -GaN nor to  $p$ -ZnO materials [9]. If the spectra reported in [3,9] certainly originate from the tunnel emission, it is the evidence for negligible non-radiative carrier recombination produced by the III-N/ZnO interfaces.

The internal quantum efficiency (IQE) as a function of current density is plotted in Fig.2a for both SHS LEDs. Here, IQE is the ratio of the radiative recombination rate integrated over the structure to the

total carrier flux  $j/q$ , where  $j$  is the current density and  $q$  is the electron charge. Being defined in such a way, IQE accounts not only the competition between the radiative and non-radiative recombination but also the carrier leakage from the structure. It is seen from Fig.2a that in the practically interesting range of the current density variation, 1-1000 A/cm<sup>2</sup>, IQEs of both SHS are comparable with each other.

In contrast to III-nitride devices (see, e.g., [7]), IQE of hybrid SHS LEDs does not grow with current density (Fig.2a) that is partly caused by insufficient suppression of the carrier leakage, i.e. losses of the minority carriers at the contact electrodes. This drawback can be eluded by using DHS LEDs where the non-equilibrium carriers become well confined in an active region due to wide-bandgap stopper layers.

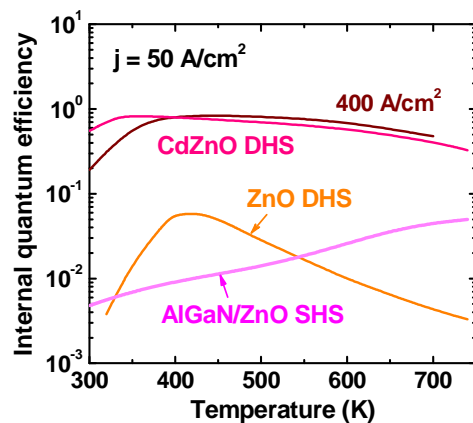


**Fig.2** IQE as a function of current density computed for SHS (a) and DHS (b) hybrid LEDs. Operation temperature of 390 K corresponds to IQE maximum of the ZnO DHS structure (see Fig.3).

**Double-heterostructure LEDs** A typical hybrid DHS LED reported in [4,5] consists of a 0.8  $\mu\text{m}$   $p$ -GaN contact layer ( $p \sim 10^{17} \text{ cm}^{-3}$ ), a 40 nm  $p$ -Al<sub>0.16</sub>Ga<sub>0.84</sub>N stopper layer ( $p \sim 10^{17} \text{ cm}^{-3}$ ), a 40 nm unintentionally doped ZnO active layer ( $n \sim 10^{17} \text{ cm}^{-3}$ ) followed by a 40 nm  $n$ -Mg<sub>0.1</sub>Zn<sub>0.9</sub>O stopper layer ( $n \sim 10^{17} \text{ cm}^{-3}$ ) and a 10 nm  $n$ -Mg<sub>0.1</sub>Zn<sub>0.9</sub>O contact layer ( $n \sim 4 \times 10^{18} \text{ cm}^{-3}$ ), all grown by molecular beam epitaxy. Recently CdZnO has been suggested as a promising active region material for visible light emitters [11]. We consider here a prototype of such LED that differs from the above structure by a 200 nm  $n$ -ZnO contact layer ( $n = 1 \times 10^{19} \text{ cm}^{-3}$ ) and an undoped 10 nm Cd<sub>0.07</sub>Zn<sub>0.93</sub>O quantum well (QW) sandwiched between the  $p$ -AlGaIn and  $n$ -MgZnO stopper layers. The use of the QW is expected to increase the concentration of the injected carrier and thus to improve IQE of the heterostructure. The former and the latter structures are hereafter referred to as ZnO DHS and CdZnO DHS, respectively. The operation of the DHS LEDs is simulated, assuming the Ga(Zn)-polarity of the crystal and TDD of  $2 \times 10^8 \text{ cm}^{-2}$  in accordance with estimate of Ref.[5].

Computed band diagrams and carrier concentrations of the DHS LEDs at  $j = 50 \text{ A/cm}^2$  are shown in Fig.1c,d. As in SHS LEDs, the built-in polarization charges induce the carrier localization next to the structure interfaces. Nevertheless, the active region bulk is found to provide a major contribution to the emission spectra due to a higher concentration of non-equilibrium carriers. The DHS LEDs exhibit remarkably higher IQE compared to the SHS LEDs (Fig.2b). Especially pronounced the IQE improvement is in the CdZnO DHS owing to larger band offsets at the stopper layer interfaces and a reduced active region thickness.

**Temperature effects** The temperature-dependent IQEs of various hybrid SHS and DHS LEDs corresponding to the current density of  $50 \text{ A/cm}^2$  are plotted in Fig.3. It is surprising that the maximum IQEs of the DHS LEDs are reached in the range of 380–420 K rather than at room temperature. In turn, the IQE of the AlGaIn/ZnO SHS is found to increase monotonically with temperature up to 700 K. On the basis of simulations, we attribute the IQE improvement at high-temperature operation to redistribution of the LED band diagrams in such a way, as to increase the heights of the potential barriers formed in the



AlGaIn layers and, hence to suppress the carrier leakage from the heterostructures. As the electron leakage is more crucial than the hole one because of very different carrier mobilities, the same effect is also responsible for the IQE increase with temperature in the AlGaIn/ZnO SHS.

**Fig. 3** Temperature-dependent IQEs of hybrid LEDs at  $j = 50 \text{ A/cm}^2$ . IQE of CdZnO DHS at  $400 \text{ A/cm}^2$  is also plotted for comparison.

Fig.3 also demonstrates that in the temperature range of 400-450 K the AlGaIn/ZnO SHS provides the IQE up to  $\sim 1\%$ , while the IQEs of the ZnO DHS and CdZnO

DHS become as high as  $\sim 6\%$  and  $\sim 80\%$ , respectively. That IQE of a DHS is systematically higher than that of an SHS, can be explained by improvement of the carrier confinement in the active region of the DHS and, hence, suppression of the leakage current. It is interesting that the CdZnO DHS provides IQE of  $\sim 80\text{--}85\%$  both at a low ( $50 \text{ A/cm}^2$ ) and a high ( $400 \text{ A/cm}^2$ ) current density. This value is comparable with the theoretically predicted IQE of conventional blue III-nitride LEDs.

**Conclusion** We have considered by modelling specific mechanisms involved in operation of SHS and DHS hybrid II-O/III-N LEDs. Band diagrams of such devices controlled by both type-II band alignment at the ZnO/III-N interface and polarization charges provide IQE having a maximum at 375-420 K that is advantageous for high-temperature LED operation. The IQE is largely affected by the carrier leakage from the diode, which can be suppressed in DHS with wide-bandgap stopper layers confining electrons and holes in the active region. A high IQE,  $\sim 80\%$ , is predicted to be attained in a DHS with a CdZnO QW active region. The efficiency corresponds to the theoretical estimates of IQE of conventional blue III-nitride LEDs, which opens opportunities for practical applications of the hybrid LEDs.

**Acknowledgements** The work of K. A. Bulashevich was supported in part by the Russian Federal Program on Support of Leading Scientific Schools and Russian Foundation for Basic Research (grant 05-02-16679).

## References

- [1] Ü. Özgür, Ya. I. Alivov, C. Liu, A. Teke, M. A. Reshchikov, S. Doğan, V. Avrutin, S.-J. Cho, and H. Morkoç, *J. Appl. Phys.* **98**, 041301 (2005).
- [2] D. C. Look, *Semicond. Sci. Technol.* **20**, 555 (2005).
- [3] Ya.I. Alivov, E.V. Kalinina, A.E. Cherenkov, D.C. Look, B. M. Ataev, A.K. Omaev, M.V. Chukichev, and D.M. Bagnall, *Appl. Phys. Lett.* **83**, 4719 (2003).
- [4] A. Osinsky, J. W. Dong, M. Z. Kauser, B. Hertog, A. M. Dabiran, C. Plaut, P. P. Chow, S. J. Pearton, X.Y. Dong, and C. J. Palmstrøm, *Electrochem. Soc. Proc.* **2004-6**, 70 (2004).
- [5] J. W. Dong, A. Osinsky, B. Hertog, A. M. Dabiran, P. P. Chow, Y. W. Heo, D. P. Norton, and S. J. Pearton, *J. Electron. Mat.* **34**, 416 (2005).
- [6] S.-K. Hong, T. Hanada, H. Makino, Y. Chen, H.-J. Ko, T. Yao, A. Tanaka, H. Sasaki, and S. Sato, *Appl. Phys. Lett.* **78**, 3349 (2001).
- [7] K. A. Bulashevich, V. F. Mymrin, S. Yu. Karpov, I. A. Zhmakin, and A. I. Zhmakin, *J. Comput. Phys.* **213**, 214 (2006).
- [8] I. Vurgaftman, J. R. Meyer, and L. R. Ram-Mohan, *J. Appl. Phys.* **89**, 5815 (2001).
- [9] D.-K. Hwang, S.-H. Kang, J.-H. Lim, E.-J. Yang, J.-Y. Oh, J.-H. Yang, and S.-J. Park, *Appl. Phys. Lett.* **86**, 222101 (2005).
- [10] K. A. Bulashevich, I. Yu. Evstratov, V. N. Nabokov, and S. Yu. Karpov, *Appl. Phys. Lett.* **87**, 243502 (2005).
- [11] S. Y. Ham, H. Yang, D. P. Norton, S. J. Pearton, F. Ren, A. Osinsky, J. W. Dong, B. Hertog, and P. P. Chow, *J. Vac. Sci. Technol.* **B24**, 690 (2006).